Archives of Materials Science and Engineering

Volume 77
Issue 1
January 2016
Pages 12-30

International Scientific Journal
published monthly by the
World Academy of Materials
and Manufacturing Engineering

The influence of reduced graphene oxide on the structure of the electrodes and the properties of dye-sensitized solar cells

L.A. Dobrzański, M. Prokopiuk vel Prokopowicz*
Division of Materials Processing Technology, Management and Computer Techniques in Materials Science, Institute of Engineering Materials and Biomaterials, Silesian University of Technology, ul. Konarskiego 18a, 44-100 Gliwice, Poland
* Corresponding e-mail address: marzena.prokopiuk@polsl.pl

ABSTRACT

Purpose of the paper: The aim of the research is to investigate the influence of the structure and chemical composition of the surface layers containing reduced oxide graphene on the properties of dye-sensitized solar cells, and to determine the correlation between the morphology and physicochemical properties of reduced graphene oxide and the electrical and optical properties of dye-sensitized solar cells, which will result in the desired effects - reducing production costs and increasing the efficiency of dye cells.

Design/methodology/approach: Complete manufacturing technology of dye-sensitized solar cells included the selection of the conditions of the thermal reduction of graphene oxide, the development of manufacturing technology of photoanode with and without reduced graphene oxide, the development of manufacturing technologies of counter electrodes with the reduced graphene oxide and the production of dye-sensitized solar cells by combining photoanode and counter electrode and filling the space between them by the electrolyte.

Findings: A reduced graphene oxide layers applied to a glass substrate with transparent conductive oxide, used as a counter electrode and photoanode effect on reducing the degree of recombination and increasing electrochemical properties, which makes them important factors in increasing the efficiency of photovoltaic cells and reduce their manufacturing costs.

Research limitations/implications: Dye-sensitized solar cells research develop in the direction to increase their efficiency and reduce manufacturing costs, among others, by modifying the chemical composition and structure of the main components: photoanode and counter electrode. Using one of the most expensive materials in the world - a platinum as a catalytic layer causes a significant increase in production costs. For this reason, it is important to search for new materials that can replace the expensive platinum.

Practical implications: Developed in this work producing technology of photoanode and the counter electrode containing reduced graphene oxide is an attractive alternative to dye-sensitized solar cell by reducing the manufacturing cost by eliminating costly layer of platinum while maintaining a relatively high efficiency, high transmittance and low resistance of charge transfer at the interlayer counter electrode/electrolyte.

Originality/value: In the paper, the reduced graphene oxide was applied as both photoanode and the counter electrode in dye-sensitized solar cells.

Keywords: Dye-sensitized solar cells; Counter electrode; Photoanode; Reduced graphene oxide

Reference to this paper should be given in the following way:

L.A. Dobrzański, M. Prokopiuk vel Prokopowicz, The influence of reduced graphene oxide on the structure of the electrodes and the properties of dye-sensitized solar cells, Archives of Materials Science and Engineering 77/1 (2016) 12-30.

PROPERTIES

1. Introduction

The technological progress causes a continuous increase in demand for electricity. Humanity consumes large energy resources, and most of the energy comes precisely from fossil sources (Fig. 1). Energy consumption is estimated to double up to 2050 [1-3], and thus increase the level of exploitation of fossil fuels like coal and lignite, oil and natural gas [4-6]. According to forecasts, fossil fuel resources may be depleted over the next few years [7-9]. The problem arising from the use of conventional energy is also the emission of environmentally harmful gases: CO_2, SO_2, NO_2, NO_x [8]. It was estimated that a safe concentration of carbon dioxide in the atmosphere that does not endanger civilization and life in a form in which they currently exist on the Earth, is 350 ppm [10], although the present carbon dioxide concentration is 395 ppm and is increased by 2 ppm per year [10]. It causes undesirable effects in the form of acid rain, global warming and severity of catastrophic events [2,7]. The growth of environmental awareness is one of the main factors driving the search for unconventional and environmentally friendly energy sources. Among them, photovoltaic energy [11,12], which in comparison with other renewable energy sources has the potential to able to cover even the total demand of humanity for electricity [12-14] plays a very important role.

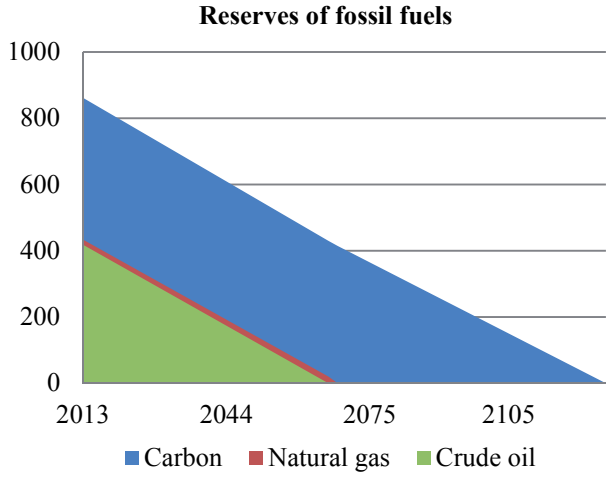

Fig. 1. World reserves of fossil fuels [8]

The dominant role in photovoltaic PV is played by crystalline silicon photovoltaic cells belonging to the first generation of photovoltaic cells, which constitute more than 80% of the PV market [15-17], but their main disadvantage is the very high cost of production compared with conventional sources of electricity [6,18]. For this reason, there are ongoing intensive research on alternative types of photovoltaic cells, which can contribute to lower the cost of their production [19-22]. Currently, the most promising is the third generation of photovoltaic cells [19,21] which include dye-sensitized solar cells [13,23]. In 1991, a team of Professor Michael Grätzel from the Federal University of Lausanne published in the "Nature" journal groundbreaking work, in which he presented the structure and operation of the dye-sensitized solar cells DSSCs, with an efficiency of 7.1%.

Dye-sensitized solar cells, also called the Grätzel cells represent the third generation of photovoltaic cells based on organic compounds which do not have the p-n junction which is typical for first and second generation. Dye-sensitized solar cells contain special chemicals compounds capable to capturing solar radiation photons and convert them into electricity.

Numerous advantages of dye-sensitized solar cells include: much higher aesthetics compared to the first generation solar cells, low toxicity, high transmittance, the possibility of colors selection, simplicity of manufacturing and low sensitivity to the angle of incidence of solar radiation [24-26]. The high transmittance makes it possible to use those cells in building integrated photovoltaics BIPV [27,28], which is an important element of the development concept of a modern, environmentally and user friendly architecture. The dye-sensitized solar cell, due to the possibility of using flexible substrates, can be used as elements of clothing, bags, tents, serving as a power source

of portable electrical equipment such as laptops or mobile phones. The operation under reduced sunlight and low impact of angle of incidence light on solar cells efficiency allows for the use of those cells in cars powered by solar energy [29]. Conventional dye-sensitized solar cell consists of two glass substrates covered by a layer of transparent conductive oxide TCO, between which is an electrolyte. One of the TCO glass coated with a catalytic material plays a role of a counter electrode and the other one, coated with titanium dioxide and the absorbed dye serves as a photoanode (Fig. 2). By modifying the chemical composition and structure of the main elements of dye-sensitized solar cells (photoanode and counter electrode), it is possible to improve the efficiency and reduce the cost of their production, and as a result they may be an alternative to a conventional silicon photovoltaic cells [20,30,31].

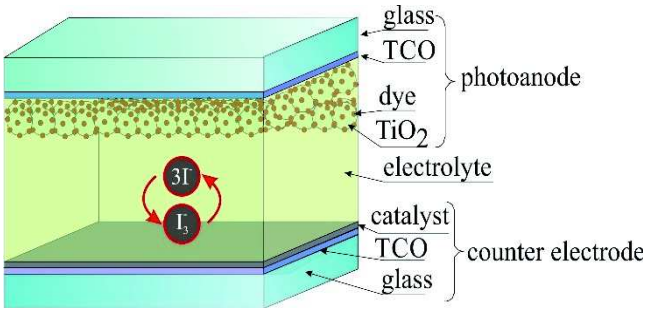

Fig. 2. Structure of dye-sensitized solar cells [13]

The improvement of electrical properties, as well as the lowering the production of dye-sensitized solar cells is associated with the optimization of each components of the solar cells. Due to the continuous development of materials engineering and nanotechnology, further realization of market demand for the dye-sensitized solar cell with increased efficiency that fulfill the economic requirements for use in industry is possible.

One of the solutions is to use nanostructured carbon, like graphene, which because of its unique electrical and optical properties can be used as [30]: electrocatalyst on the counter electrode, alone or with other functional materials, to provide an alternative to the costly nanoparticles of platinum, the filling of the electrolyte increasing conductivity [32], a nanostructured component of photoanode allowing to reduce the level of recombination of the electron with a reduced redox couple. Most of the graphene electrodes are applied to the conductive substrate with additions of the polymeric binder, however, it faces problems with the adhesion of carbon materials to the conductive glass. Therefore, the most promising path for the manufacture of cheap graphene compounds on large scale is to produce a graphene oxide by chemical oxidation and its subsequent chemical or thermal reduction (Fig. 3).

The use of the graphene oxide is also supported by the fact that it is readily dissolved in aqueous media and in polar organic solvents, facilitating its application to the substrate or mixed with other substances. It is not possible with the primary graphene which is practically not soluble in any medium [30]. In addition, it is believed that surface damage resulting from the oxidation of graphene planes are responsible for the electrocatalytic activity. Therefore, the use of graphene oxide is favorable compared to an ideal, completely reduced graphene without defects in the structure [26].

The aim of the research work is to investigate the influence of the structure and chemical composition of the surface layers containing reduced oxide graphene on the properties of dye-sensitized solar cells, and to determine the correlation between the morphology and physicochemical properties of reduced graphene oxide and the electrical and optical of dye-sensitized solar cells, which will result in the desired effect - lower production costs and increasing the efficiency of dye-sensitized solar cells. To achieve this objective, it is necessary to analyze issues related to the effects of reduced graphene oxide on the properties of dye-sensitized solar cells. Developed the following specific objectives of work [33]:

1. Development of graphene oxide reduce technology.
2. Development of production technology of counter electrode with the reduced graphene oxide on a glass substrate with a transparent conductive oxide.
3. Development of the producing technology of photoanode with titanium dioxide on the FTO glass and the development of techniques for the preparation of modified photoanode with the reduced graphene oxide and titanium dioxide on the glass substrate with a transparent conductive oxide.
4. Production of dye-sensitized solar cells by combining photoanode and counter electrode and filling the space between by electrolyte.

The basis for the implementation of the research was to develop a suitable production technology of photoanode with reduced graphene oxide and titanium dioxide and counter electrode with the reduced graphene oxide deposited on a glass substrate with a TCO. It required the preparation of a preliminary plan for the various steps to objectives achieves (Fig. 4).

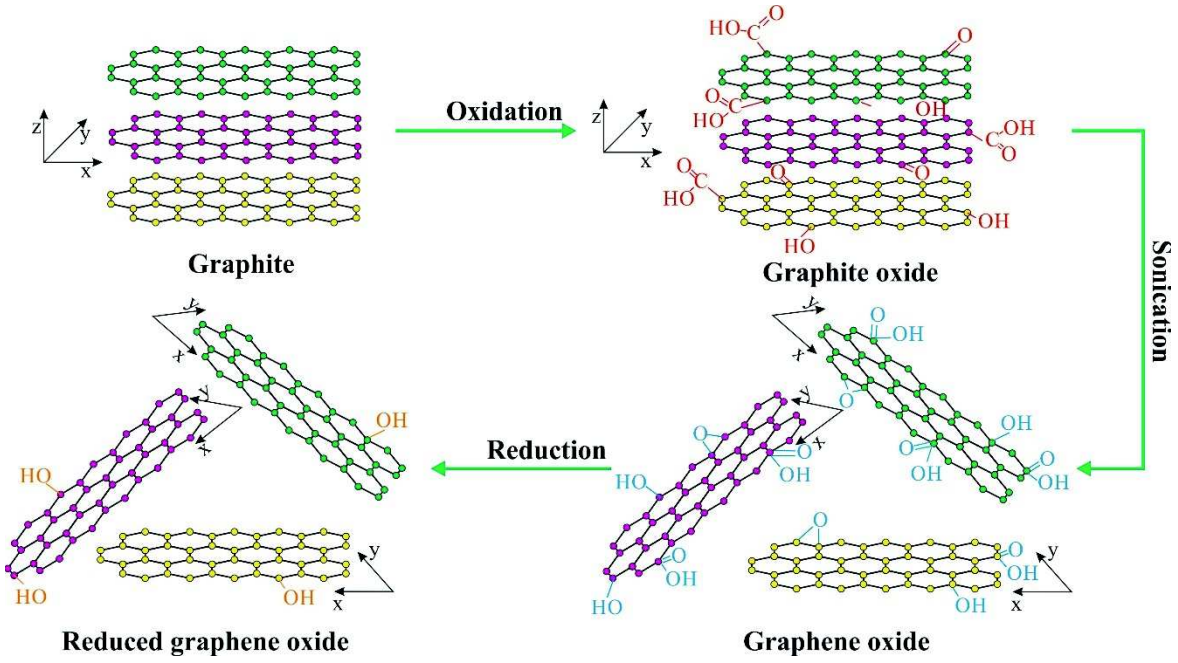

Fig. 3. The steps of reduced graphene oxide preparation by Hummers method following by thermal reduction in furnace with Ar/H_2 [30]

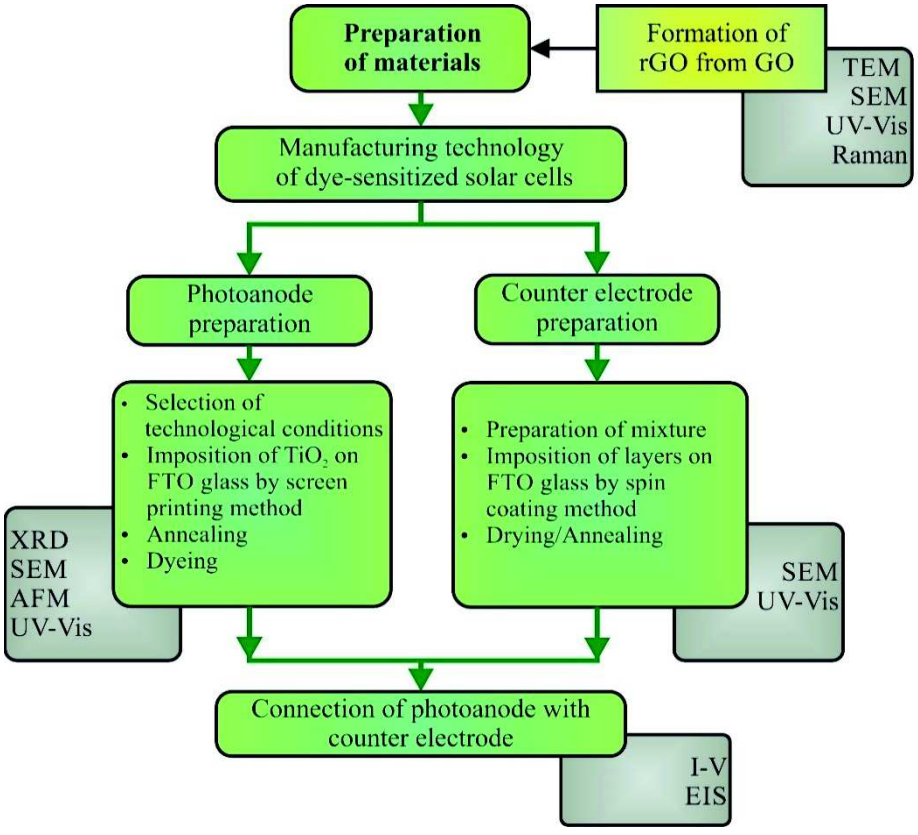

Fig. 4. The steps of research implementation [33]

2. Materials and methods

2.1. Materials

Table 1 shows the materials used in the production technology of dye-sensitized solar cells. The tests were made on glass plates with a layer of fluorine doped tin oxide, FTO (7 Ω/□, Nano 3D). The shape and dimensions of the glass plate and then applied on it the titanium dioxide layers are shown in Figure 5. In order to remove impurities, glass with transparent conductive oxide was purified by dipping and holding it for 15 min in an ultrasonic sequentially in deionized water, acetone, ethanol and at the end in isopropanol.

Table 1.
The materials used for testing

Material	Supplier	Purpose
Glass plates covered by FTO	3D Nano	Substrate
Titanium dioxide	Solaronix	Photoanode
Dye N3	Sigma Aldrich	Photoanode
PEDOT:PSS	Sigma Aldrich	Counter electrode
PVP	Sigma Aldrich	Counter electrode
Graphene oxide	CheapTubes.com	Counter electrode, photoanode
Platinum paste	3D Nano	Reference counter electrode
Iodolyte Z-150	Solaronix	Electrolyte
Meltonix	Solaronix	Sealing foil
Anhydrous ethyl alcohol	Alchem	The solvent for dye, cleaning agent
Isopropanol, Acetone	POCH	Cleaning agent

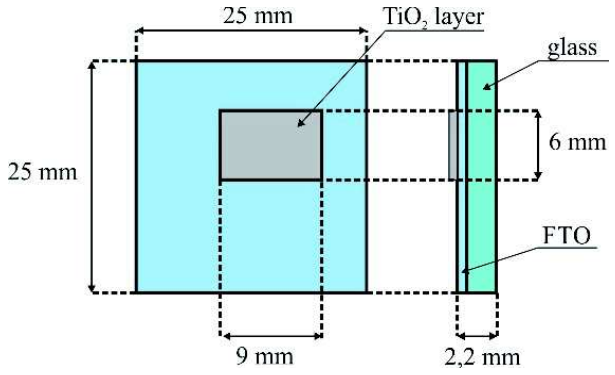

Fig. 5. The shape and dimensions of the photoanode [33]

2.2. Thermal reduction of graphene oxide

Due to the poor electrical properties of the graphene oxide it is subjected to further transformation. The most commonly used technique for the reduction of graphene oxide treats an aqueous slurry of graphite oxide produced by Hummers method by hydrazine solution. Due to the toxicity of the solution researches have been looking for new solutions. One of it is the thermal reduction of graphene oxide at a temperature higher than 250°C in inert gas containing hydrogen. In this paper, the thermal reduction of graphene oxide in a high temperature oven at 500°C for 30 minutes in inert gas Ar with H_2 in the ratio of 93:7 was applied. In the first stage an aqueous suspension of graphene oxide was dried for 36 h in a vacuum freeze dryer. Then, the resulting powder is placed in a combustion boat. The sample was annealed in an oven at 500°C and is designated as RGO. In earlier work in the team headed by Prof. LA. Dobrzański [34] the thermal reduction of graphene oxide at a temperature of 250°C and 500°C has been fulfilled. Further studies of electrochemical properties have shown that the improved catalytic properties of the redox reaction are characterized by a reduced graphene oxide thermally reduced at 500°C.

2.3. Photoanode preparation

In order to reduce the numbers of layers made from titanium dioxide, Hartley experiment plan was used. The basic plan assumed perform of 11 experiments. Adopted variable factors is (Fig. 6) [33]:

- layer thickness d (5, 10, 15 μm),
- annealing temperature T_W (300, 400, 500°C),
- annealing time t (15, 30, 45 min).

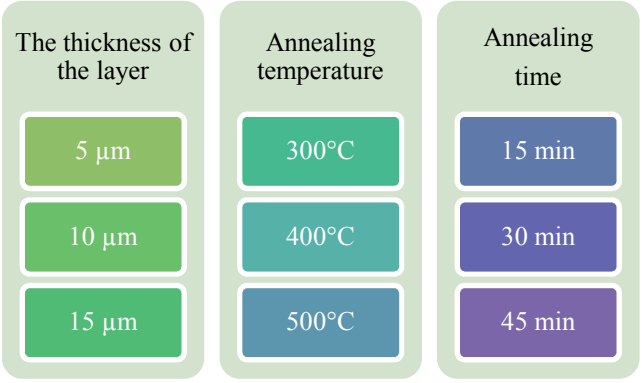

Fig. 6. Changing the production conditions of titanium dioxide layers [33]

A series of 11 experiments for the selection of the appropriate thickness, temperature and heating time of TiO_2 layer on the glass substrate with FTO layer was prepared. 1, 2 or 3 layers of titanium dioxide by screen printing method was applied on substrate with a layer of FTO and then annealed in an oven at 300°C, 400°C or 500°C for 15, 30 or 45 min. Titanium dioxide layers was applied by a universal semi-automatic screen printers MS300FRO, which is shown in Figure 7.

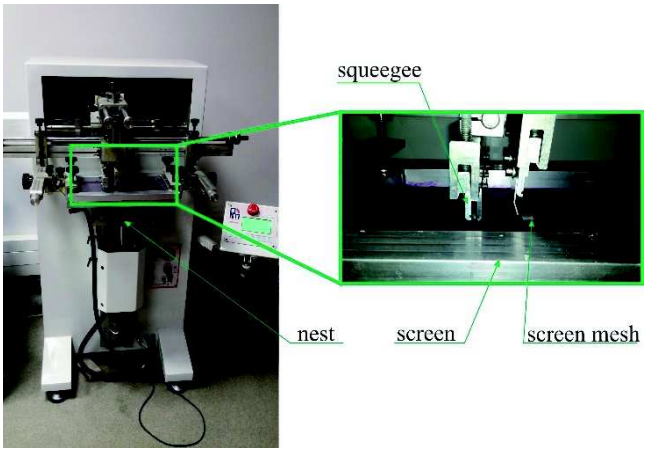

Fig. 7. Screen printer MS300FRO

The electrodes were annealed in a high temperature oven at various temperatures with a small temperature rise (30°C per minute) and holding at the temperature for 15, 30 or 45 min. The heat source was then turned off and allowed to cool to <100°C. An attempt to draw the substrate from the oven when the temperature is higher than 200°C causes thermal shock and cracking.

Based on the assessment of visual quality of the layers of titanium dioxide, as well as preliminary tests including measurement of surface roughness determined conditions of applying layers by screen printing and calcination. The best properties of layer with titanium dioxide is achieved to 3 layers which was annealed at 500°C for 30 min. Lower temperatures do not provide adequate removal of organic components which manifests itself in yellow layer, the lower the transmittance and a lower surface roughness.

In order to produce photoanode with titanium dioxide and reduced graphene oxide to the paste of titanium dioxide was added 5 wt.% of reduced graphene oxide. Properly prepared paste was applied on the FTO glass by using a screen printing method, dried, and re-applied to form three layers. Then layers were annealed in an oven at 500°C for 30 min.

After cooling to 80°C, nonstructural layer of titanium oxide and titanium oxide with a reduced graphene oxide was immersed in the dye solution. The electrode is dyed after calcination, because then it does not absorb ambient moisture. Moreover, the porous electrode with a titanium dioxide is easily contaminated with volatile substances. As the dye was used commercially available ruthenium complex – cis-diisothiocyanato-bis(2,2'-bipyridyl-4,4'-dicarboxylic acid) ruthenium(II), commonly known as N3, in powder form. N3 dye is known for its highly efficiently sensibilisation of titanium oxide in the visible spectrum to a wavelength of ~750 nm. In the present work 0.5 mM solution of N3 in ethanol was applied. The dyed electrode was removed from the dye solution using plastics tweezers (to prevent the trace metal impurities). The electrode was washed thoroughly with ethanol to remove excess of dye, because it may cause harmful build-up of dye molecules. Then the electrode was completely dried in inert gas.

2.4. Counter electrode preparation

In order to replace the expensive platinum layers with other materials, producing technology of counter electrode without platinum was developed. Reduced graphene oxide was applied as the main material for the research. However, preliminary studies have shown its poor electrical properties. Therefore, to choose the best conductive polymeric material was made an analysis using a matrix of dendrochronologically technology, introduced in [35-38]. The following materials were considered: Poly(3,4-ethylenedioxythiophene)-poly(styrenesulfonate) - PEDOT:PSS, Poly[2-methoxy-5-(2-ethylhexyloxy)-1,4-phenylenevinylene] – MEH-PPV, Poly(3,4-ethylenedioxythiophene) – PEDOT, Polypyrrole – PPy, polyaniline – PANI. for assessing the potential and attractiveness of the various materials there were matched specific criteria shown in Table 2. Based on the performed analysis (Fig. 8) for further study polymer PEDOT:PSS was selected.

Furthermore, counter electrode with reduced graphene oxide and PEDOT:PSS has numerous agglomerates. Therefore, in order to prevent aggregation of the reduced graphene oxide in the present studies to the counter electrode was added a poly(vinylpyrrolidone) – PVP, according to [38]. Optimal active material was estimated to 95 wt.%, and the optimal layer thickness to 20 μm for optimum electrochemical properties while maintaining the transmittance of the layer above 70% at a wavelength of 550 nm. Catalyst layer was made in the following volume ratio (Fig. 9) [33]:

- 95 wt.% of reduced graphene oxide, 5 wt.% PVP, marked as rGO + PVP,

Table 2.
The detailed criteria for assessing the potential and attractiveness of the material groups tested by materials-heuristic analysis

No.	Potential (objective values)	Scales
Criterion 1	The probability of development in the research area (the ability to improve properties, the existing state of knowledge)	0.3
Criterion 2	Popularity among researchers in the last decade (base on the number of publications)	0.2
Criterion 3	Toxicity	0.2
Criterion 4	Price	0.1
Criterion 5	Small degree of complexity of production technology	0.2
No.	Attractiveness (subjective values)	Scales
Criterion 1	Versatility of application due to the properties	0.3
Criterion 2	Easy to store	0.2
Criterion 3	The possibility of application of the material in the sector of small and medium-sized enterprises	0.2
Criterion 4	Market demand	0.1
Criterion 5	Material availability	0.2

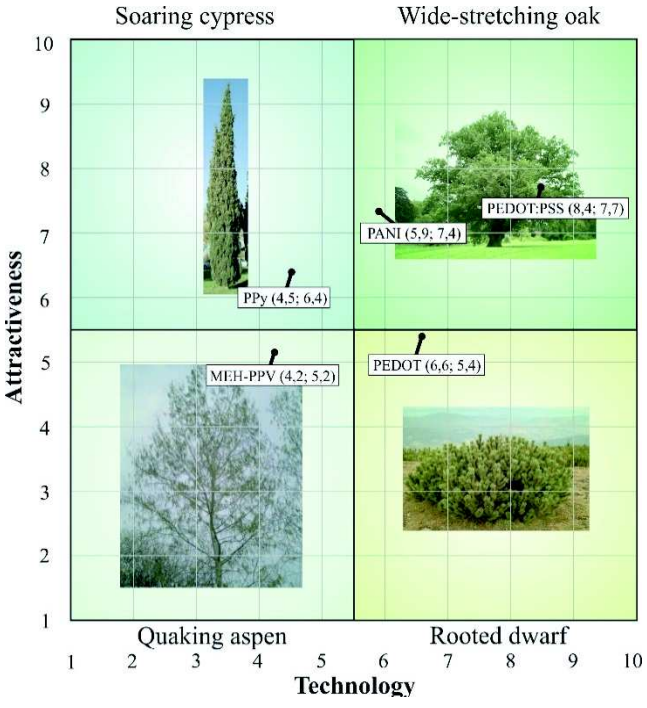

Fig. 8. Dendrological matrix of technology made for different types of conductive polymer materials usable in the production of dye-sensitized solar cells [35-38]

- 95 wt.% reduced graphene oxide with PEDOT:PSS (50 wt.% reduced graphene oxide, 50 wt.% PEDOT:PSS), 5 wt.% PVP, marked as rGO+PVP + PEDOT:PSS,
- 95 wt.% reduced graphene oxide, 5 wt.% PVP, then applied on the surface PEDOT:PSS, marked as rGO + PVP/PEDOT:PSS.

In addition, for comparison purposes also they were used subsequent counter electrode:

- platinum,
- carbon nanotubes with PVP and PEDOT:PSS,
- PEDOT:PSS.

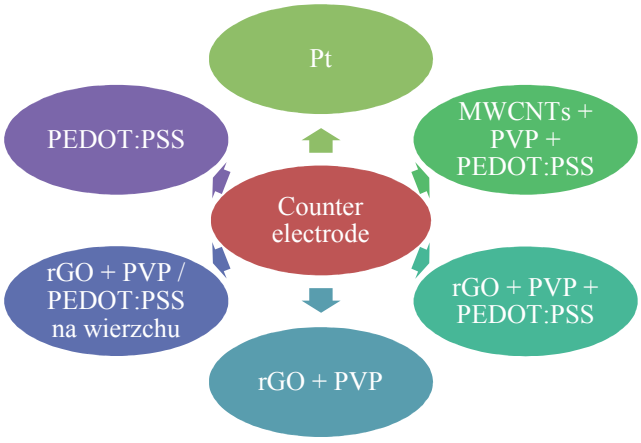

Fig. 9. Catalytic layers used as a counter electrode in dye-sensitized solar cells [33]

The manufacturing steps of the counter electrode with carbon materials is shown in Fig. 10. In order to obtain a uniform layer over the entire surface of the FTO glass, mixtures of polymers with reduced graphene oxide is applied onto a substrate by the use of the spin coating method. The layers were applied in the following stages:

- initial spin coating with 500 rpm for 5 seconds,
- spin coating with 1000 rpm for 30 seconds.

Counter electrode with catalytic layer of platinum with a Platisol paste was prepared. On previously cleaned substrate a platinum paste was applied using a screen printing method. In order to obtain the optimum thickness of the catalytic layer, 3 layers were applied. Then the counter electrode was fired at 500°C for 30 min to remove organic products and form the active layer of platinum. Results of studies on the use of screen printing techniques for the preparation of a platinum counter electrode is shown in [39].

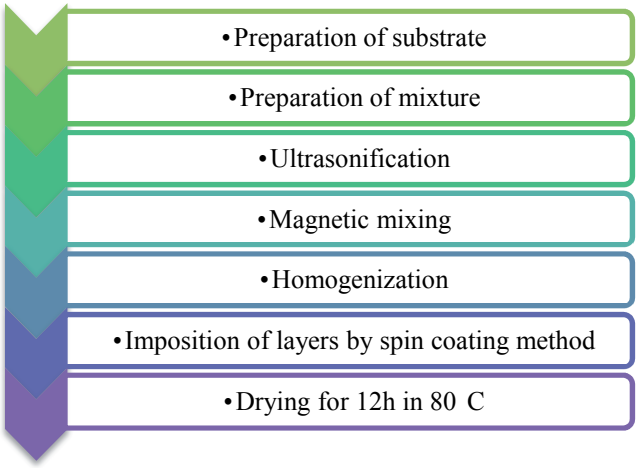

Fig. 10. Preparation steps of the catalytic layers with the reduced graphene oxide

2.5. Connection of photoanode with counter electrode

Dye-sensitized solar cells were made in 12 configurations with different material used as photoanode and counter electrode, what is shown in Figure 11.

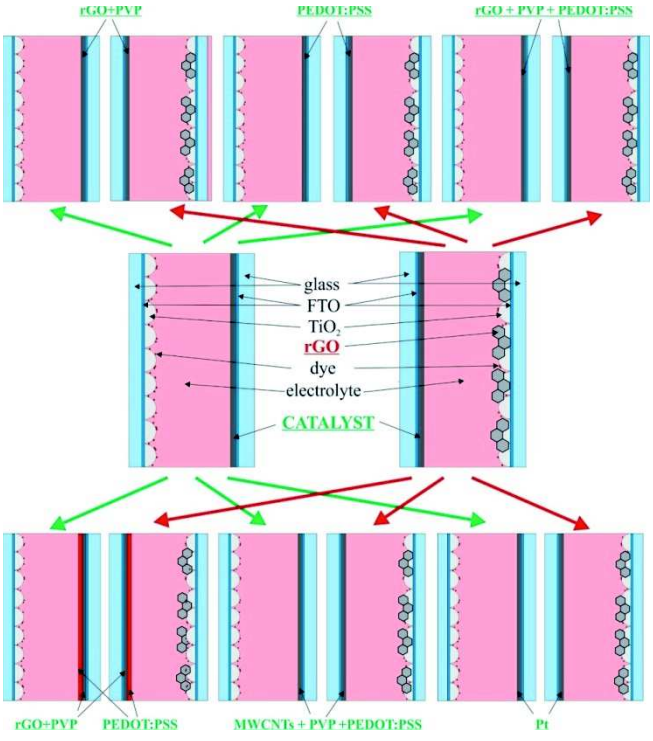

Fig. 11. Dye-sensitized solar cells made in the present work

Ready-cell was formed by combining an anode and a cathode with a Meltonix sealing film with thickness equal 25 µm, which simultaneously serves as a distance between the electrodes to prevent shorting. Sealing temperature was 100°C.

The space between the electrodes was filled with electrolyte, which was a high-performance electrolyte with a high concentration of triiodide – Iodolyte by Solaronix.

2.6. Methodology

Studies of the structure of the materials used to form the counter electrode and photoanode were performed using: Scanning Electron Microscope SEM Zeiss Supra 35, Transmission Electron Microscope S/TEM Titan 80-300 by FEI Company, inVia Raman spectrometer by Renishaw equipped with an argon ion laser with 514.5 nm excitation line and a maximum power of 50 mW, X'Pert Pro PANalytical X-ray diffractometer. The surface topography of structure of the prepared layers of dye-sensitized solar cell were made using: Scanning Electron Microscopy, Atomic Force Microscopy AFM XE-100 Park Systems. The optical properties of prepared layers were performed by using a Spectrophotometer Evolution 220 by Thermo Scientific company.

The studies of electrical properties of experimentally prepared dye-sensitized solar cells containing in its structure reduced graphene oxide were performed on a computerized station SS IV CT-02 for measurement of current-voltage (IV) characteristics of photovoltaic cells equipped with a sunlight simulator working in AAA class measurement (determined in accordance with IEC 60904-09) and with low current meter – Keithley 2401 for dye-sensitized photovoltaic cells measuring. Studies of electrochemical properties were performed using Electrochemical Impedance Spectroscopy EIS. Measurements of electrochemical impedance spectroscopy were performed using a potentiostat-galvanostat coupled to an impedance meter 0531 EU & ATLAS IA.

3. Results and discussion

3.1. Analysis of the results of reduced graphene oxide studies

A reduced graphene oxide layers are highly wrinkled and bent (Fig. 12a,b), which indicates on a residual group of oxygen after the thermal reduction. The reduced

graphene oxide has highly defected structure compared to graphene oxide, which can be explained by the removal of some of the functional groups on the edges of the plane of the graphene oxide during the thermal reduction (Fig. 12c, d). Interplanar distances amounting to 0.41 nm for the reduced graphene oxide and 0.35 nm for the graphene oxide before reduction indicates on more defected structure (Fig. 12), which can be explained by the removal of some of the functional groups on the edges of the plane of the graphene oxide.

The presence of graphene oxide and reduced graphene oxide was confirmed by identifying four bands: D, G, 2D and D + D` by Raman spectroscopy (Fig. 13a). The spectra of both graphene oxide and reduced graphene oxide were characterized by the presence of G and D bands, which indicate the existence of graphene oxide. High D-band (1350 cm^{-1} for graphene oxide and reduced graphene oxide) (Fig. 13a) indicates on defect in graphene and is a consequence of structure disorder. High intensity of D-band (Fig. 13a) indicates on a defect in graphene structure

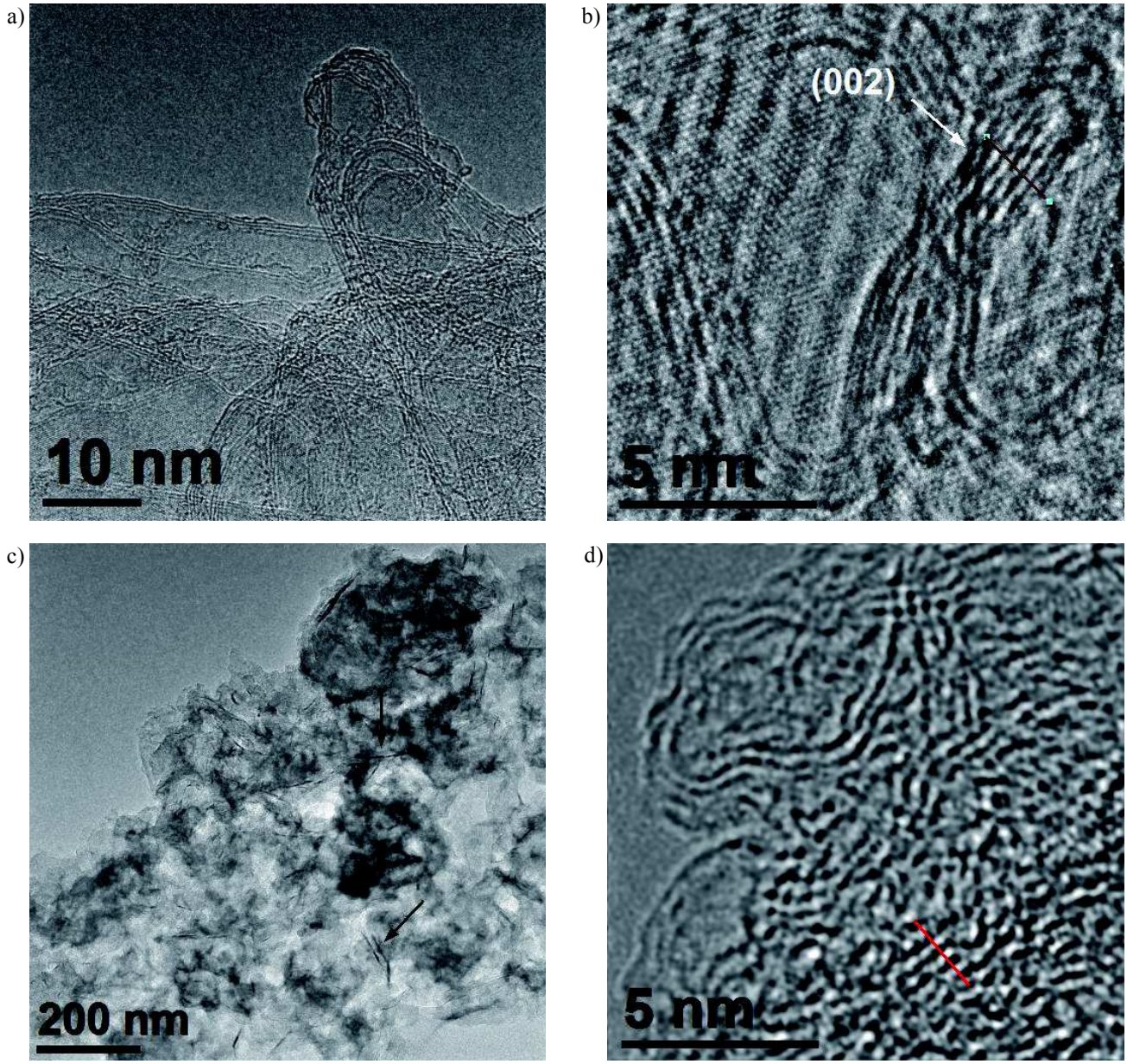

Fig. 12. The TEM images of the structure of a) and b) graphene oxide, c) and d) reduced graphene oxide

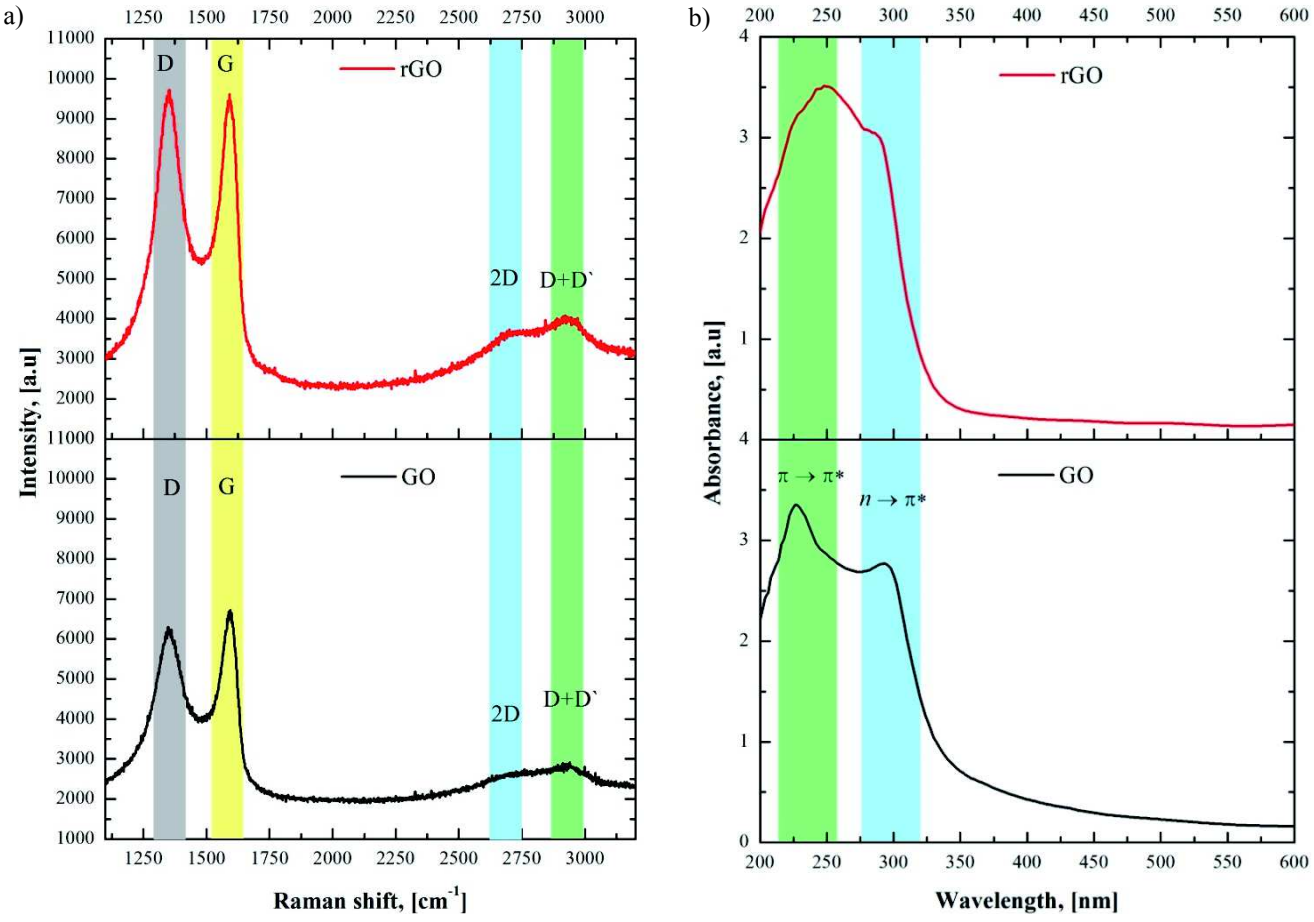

Fig. 13. Graphene oxide before and after reduction a) Raman spectrum, b) absorbance spectrum

by modifying the structure by hydroxyl and the epoxy groups substituted in basal plane and substituted the hydroxyl groups in the edges of the plane. G-band (1595 cm^{-1} for graphene oxide and 1590 cm^{-1} for the reduced graphene oxide) (Fig. 13a) corresponds to the degree of graphitization. 2D band is attributed to overtone, while the band D + D` to combination of tones (D + G) (Fig. 13a). A small intensity for 2D band for graphene oxide and reduced graphene oxide (Fig. 13a) indicates the presence of several layers of graphene with attached oxygen groups, as well as the occurrence of the disorder of the structure.

For wavelength ~2930 nm for both the graphene oxide and reduced graphene oxide (Fig. 13a) peaks D+D` are activated by occurrence of defects.

Based on the ratio intensity of D to G band (I_D/I_G), which is the main characteristic of the disorder and measurement of the defects amount in the material, confirmed the reduction of graphene oxide. The intensity ratio of I_D/I_G for graphene oxide is 0.92, and for the reduced graphene oxide 1.03. Increasing the intensity ratio I_D/I_G for reduced graphene oxide is caused by increased disorder of the structure, due to continued tearing of flakes of graphene oxide and delamination in structures leading to the accidental deployment of the layers as a result of the thermal reduction of the graphene oxide.

In order to confirm the reduction of graphene oxide were examined the absorbance of graphene oxide and reduced graphene oxide deposited on glass. As a result of the thermal exfoliation the maximum absorption peak was bathochromic shifted from 230 nm to 250 nm (Fig. 13b). This peak corresponds to the transition of electrons from the highest occupied molecular orbital HOMO to the lowest unoccupied molecular orbital LUMO $\pi \rightarrow \pi^*$. Bathochromic shift indicates the production of a double bond C=C during the reduction, in contrast to graphene oxide where there is a single bond C-C. The presence of a second peak for wavelength equal 290 nm (for graphene oxide) and 300 nm (for reduced graphene oxide) indicates the presence of C=O bonds, in which there was a transition electron $n \rightarrow \pi^*$ (Fig. 13b).

3.2. Result analysis of photoanode structural and optical properties

The entire surface of the FTO glass is uniformly coated with the nanocrystalline titanium dioxide (Fig. 14). There was no influence of temperature, time and number of layers on the morphology of the layer. Regardless of the manufacturing conditions, there were no discontinuities and contaminants (Figs. 15, 16). The titanium dioxide particles are densely packed and have a globular shape (Fig. 16). In the case of the use of titanium dioxide with the reduced graphene oxide as photoanode of dye-sensitized solar cells there is the effect in increasing the porosity of the layer (Fig. 17). Between the reduced graphene oxide and titanium oxide there is good contact, and reduced graphene oxide is evenly distributed in the material (Fig. 17)

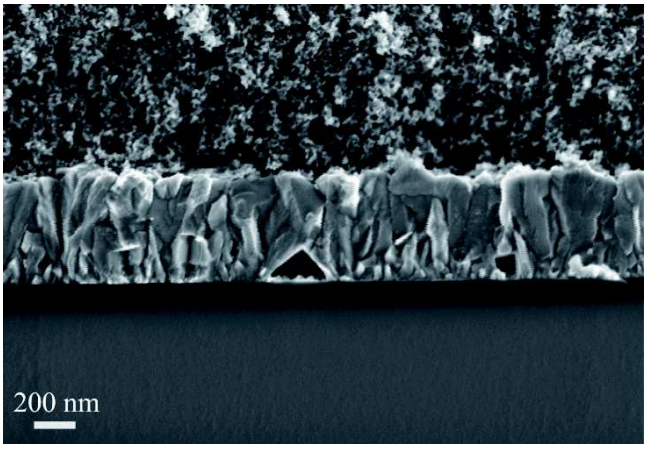

Fig. 14. The cross section of the FTO glass with a layer of titanium dioxide, SEM

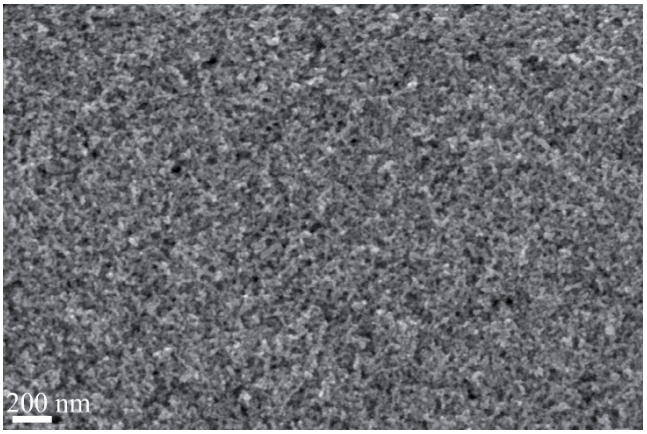

Fig. 15. The morphology of the titanium dioxide layers applied on the FTO glass and annealed at 300°C for 30 min, SEM

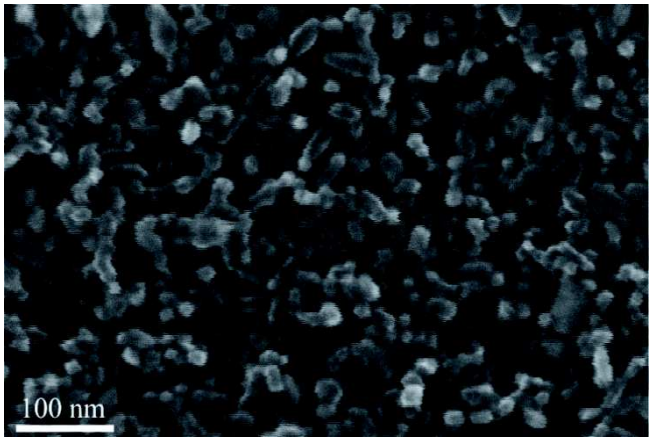

Fig. 16. The morphology of the titanium dioxide layers applied on the FTO glass and heated up at 500°C for 30 min, SEM

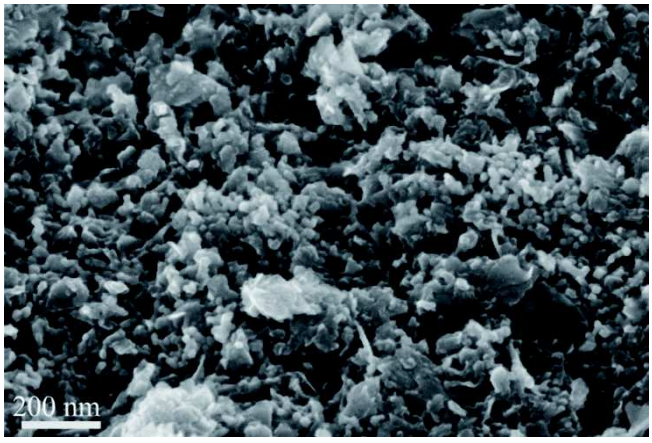

Fig. 17. The morphology of the titanium dioxide layers with reduced graphene oxide applied on the FTO glass, SEM

On the basis of studies of the surface topography and roughness on the sample scan area equal 5 mm x 5 mm, it was found out that the surfaces of the photoanode layers before dyeing (Figs. 18 and 19) is characterized by regular clusters of atoms of titanium dioxide in elliptical shape. There was no occurrence of cracks and gaps in the structure.

Titanium dioxide layers with a reduced graphene oxide have a globular structure. It was found that out that the layers with a reduced graphene oxide have larger surface area, which is 26.40 μm^2 in comparison to the layer without reduced graphene oxide (26.20 μm^2), with the test surface 25 μm^2. It means that after the introduction of the reduced graphene oxide into a paste with a titanium dioxide this coating have a higher unevenness of surface, but a more globular structure with a larger surface area (Table 3).

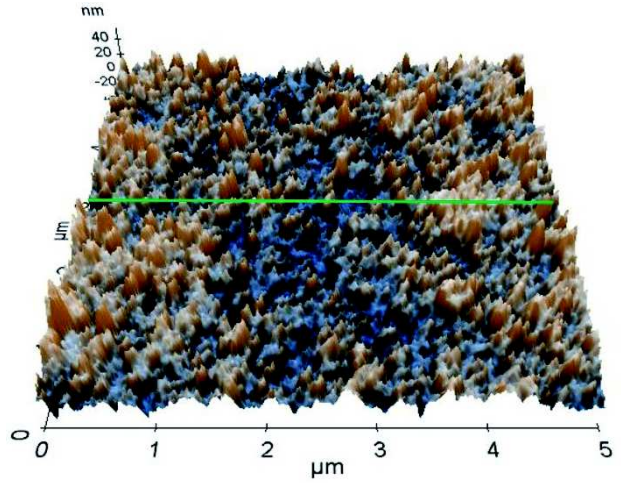

Fig. 18. 3D topographic image obtained by using an atomic force microscope for 3 layers of titanium dioxide annealed at 500°C for 30 min

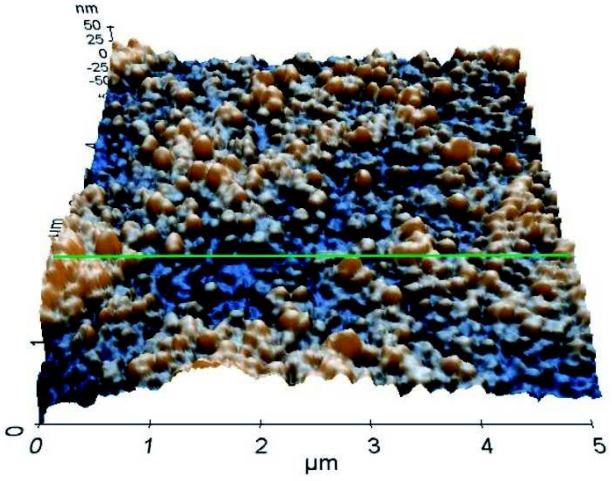

Fig. 19. 3D topographic image obtained by using an atomic force microscope for 3 layers of titanium dioxide with reduced graphene oxide annealed at 500°C for 30 min

Table 3.
Summary of selected roughness parameter for titanium dioxide and titanium dioxide with reduced graphene oxide layers deposited by screen printing method

Material	The studied area, µm^2	Surface area, µm^2	R_a, nm	R_q, nm
		Before dyeing		
TiO_2	25	26.21	8.67	10.76
TiO_2 + rGO	25	26.40	9.22	11.73
		After dyeing		
TiO_2	25	26.87	20.30	24.99
TiO_2 + rGO	25	27.82	21.63	28.68

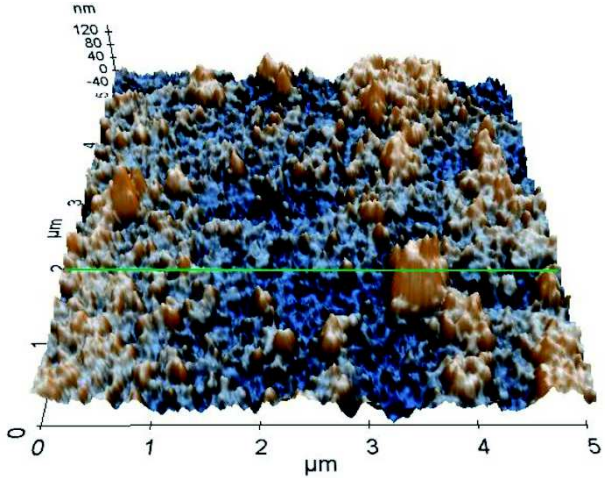

Fig. 20. 3D topographic image obtained by using an atomic force microscope for 3 layers of titanium dioxide annealed at 500°C for 30 min and then dyed

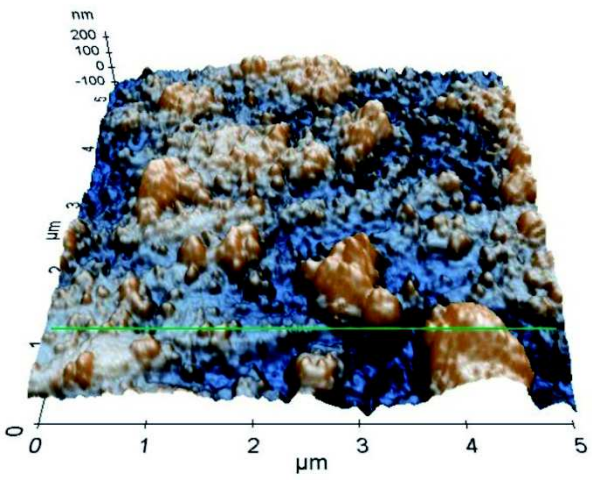

Fig. 21. 3D topographic image obtained by using an atomic force microscope for 3 layers of titanium dioxide with reduced graphene oxide annealed at 500°C for 30 min and then dyed

The addition of reduced graphene oxide into layer of titanium dioxide also influence on the increase in the surface roughness amplitude parameter R_a (arithmetic average of absolute values) from 8.67 nm to 9.22 nm and R_q (root mean squared) from 10.76 nm to 11.73 nm (Table 3).

Images of the surface of layers in the form of 3D mapping document the great differences in surface topography for the titanium dioxide layers with or without a reduced graphene oxide subjected to dyeing. After photo-anodes dyeing on the surfaces of the layers there are higher concentrations of atoms irregularly spaced (Figs. 20, 21).

Photoanode dyeing also influences the increase of surface area to 26.87 μm^2 for TiO_2 and 27.82 μm^2 for the layers with reduced graphene oxide. After the dyeing layers have larger unevenness (Table 3). Size of R_a parameter of the titanium dioxide layer after dyeing increases from 8.67 nm to 20.30 nm and from 9.22 nm to 24.99 nm for the dyed layers of titanium dioxide with a reduced graphene oxide, while R_q is equalled respectively 21.63 nm and 28.68 nm (Table 3).

No influence of temperature, time and number of titanium dioxide layers on glass with a layer of transparent conductive oxide on crystal structure and phase composition of the material was confirmed by X-ray (Fig. 22). In all cases, there the presence of anatase phase from titanium dioxide and cassiterite phase from tin dioxide originating from the FTO layer (Fig. 22) was identified. Reduced graphene oxide due to its small share in photoanode containing titanium dioxide with the reduced graphene oxide does not change the phase composition of the material.

Titanium dioxide deposited on the glass cause shifting the spectral transmittance in the direction of longer wavelengths, thereby affecting the reduction in light transmittance compared to the FTO glass and the indicates bathochromic effect of the absorption spectra. Applications of a reduced graphene oxide in photoanode of dye-sensitized solar cell increases transmittance for ultraviolet light (Fig. 23).

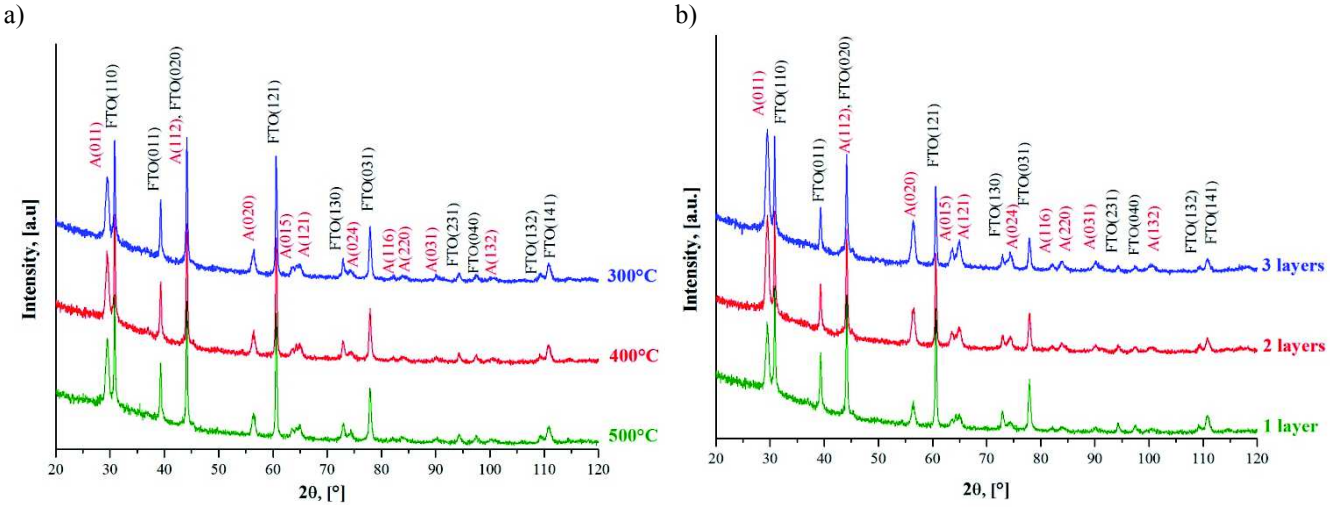

Fig. 22. X-ray diffraction pattern of the titanium dioxide layers on the FTO glass and annealed a) at 300°C, 400°C or 500°C, b) with different thicknesses deposited on the FTO glass

The application of a reduced graphene oxide in photoanode of dye-sensitized solar cell increases transmittance to 600 nm and a decrease in transmittance in the wavelength greater than 600 nm as compared to photoanode without reduced graphene oxide (Fig. 23). The reduced graphene oxide in the dyed photoanodes influence the offset of the transmission spectra in the direction of shorter wavelengths, and also reduce the maximum transmittance (Fig. 24).

Absorption of solar radiation by a molecules of dye was confirmed by absorbance. In the absorption spectrum of the dyed photoanode there are two absorption peaks in the visible light range in 400 nm and 535 nm (Fig. 25). These are two optical transitions in the visible light, which is attributed to the transfer of charge from the Highest Occupied Molecular Orbital to Lowest Unoccupied Molecular Orbital of the dye.

The use of the reduced graphene oxide affects the bathochromic shift of the absorption spectra to 700 nm as well as an increase in absorbance of dyed photoanode (Fig. 25).

By measuring the absorbance A(λ), it is possible to determine the Light Harvesting Efficiency LHE, which allows for the identification possibilities for the dye to absorb photons at different wavelengths [2]:

$$\mathrm{LHE}(\lambda) = 1 - 10^{-\mathrm{A}(\lambda)} \quad (1)$$

Dye affects the growth in the light harvesting efficiency LHE also in the visible range (Fig. 26). The use of additional

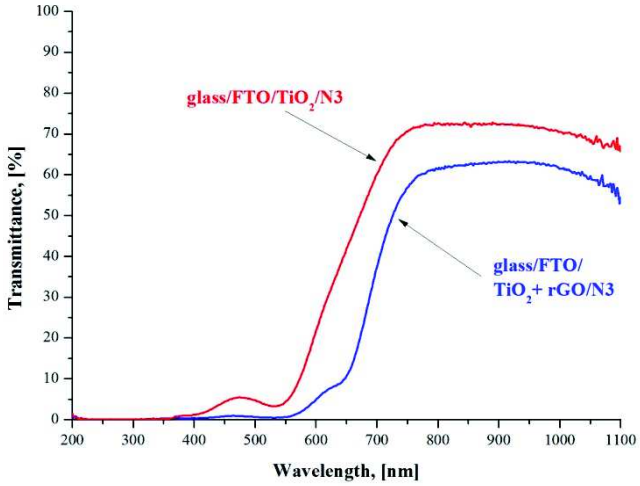

Fig. 23. Transmittance spectra of the dye-sensitized solar cell photoanode with and without reduced graphene oxide

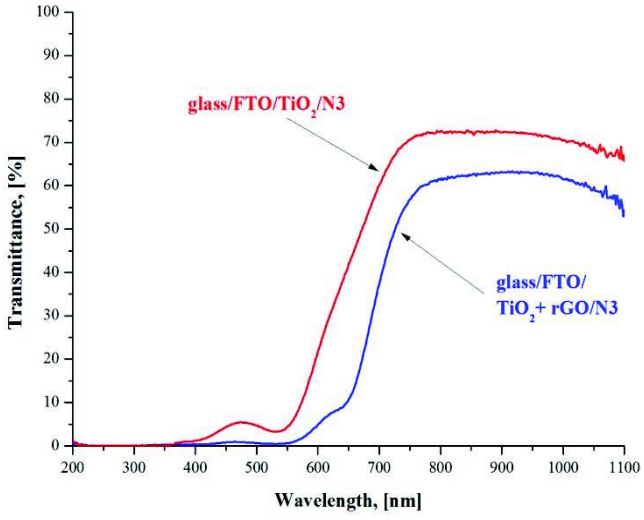

Fig. 24. Comparison of the transmittance spectra of the dyed photoanode of dye-sensitized solar cells with titanium dioxide with and without reduced graphene oxide

reduced graphene oxide in the dyed photoanode increases the efficiency of light harvesting LHE both in the ultra-violet and visible light (Fig. 26). Furthermore, photoanode with a reduced graphene oxide is able to absorb more solar radiation than photoanode without reduced graphene oxide, increasing energy conversion efficiency of solar radiation into electrical energy (Fig. 26). This is due to the fact that between the particles of titanium dioxide and the reduced graphene oxide forms two dimensional structures for faster transition of electrons to the FTO layer, and thereby reducing the degree of recombination of the excited electron with the triiodide anion of the electrolyte.

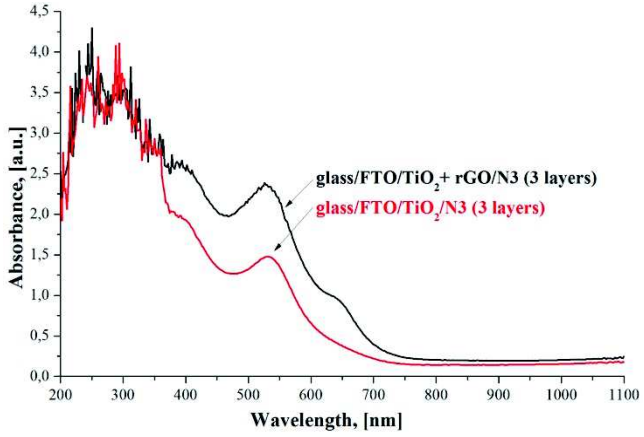

Fig. 25. Comparison of the absorption spectra of dye-sensitized solar cell photoanode for the layers of titanium dioxide with and without the reduced graphene oxide, dyed

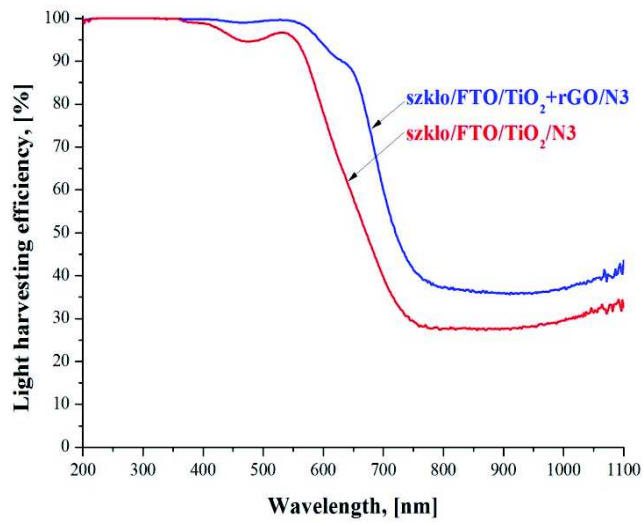

Fig. 26. Comparison of light harvesting efficiency for photoanode of dye-sensitized solar cell with and without reduced graphene oxide with absorbed dye

3.3. Analysis of the results of structural and optical properties of counter electrodes

In the deposited layers of reduced graphene oxide with polymer materials found cavities and voids (Figs. 27-29). There were no contaminants presented on the surface of the layers (Figs. 27-29). In the case of a PEDOT:PSS polymer layer coated on the surface of the reduced graphene oxide with PVP material found that reduced graphene oxide is completely covered with the conductive polymer material (Fig. 29).

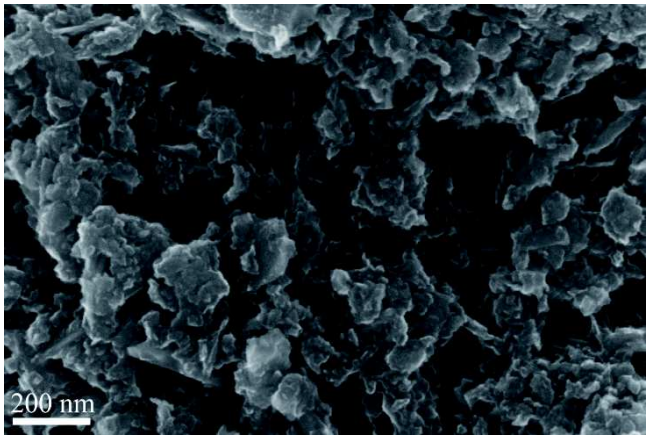

Fig. 27. The morphology of the reduced graphene oxide with PVP

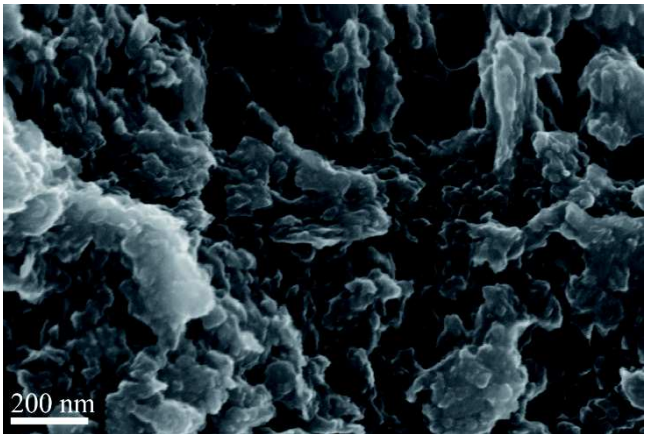

Fig. 28. The morphology of the reduced graphene oxide with PVP and PEDOT:PSS

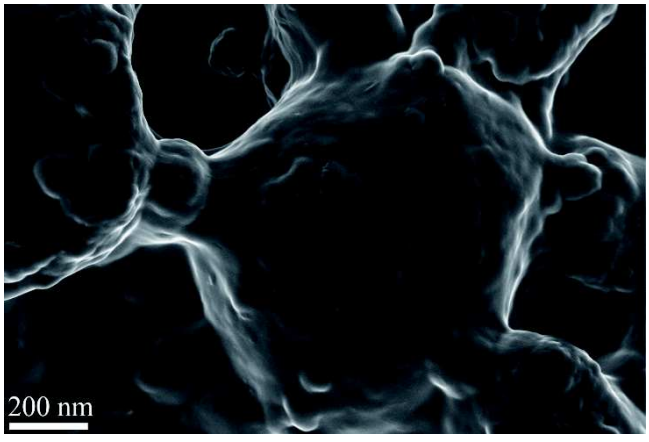

Fig. 29. The morphology of the reduced graphene oxide with PVP coated by layer of PEDOT:PSS

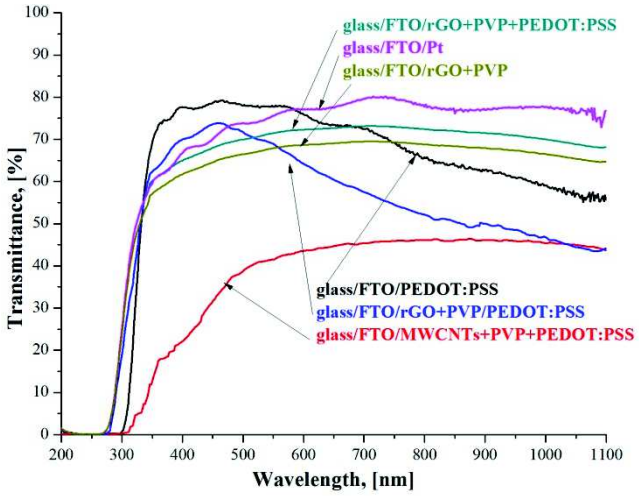

Fig. 30. Transmittance spectra of the layers used as the counter electrode in dye-sensitized solar cells

All of the catalytic layer with a reduced graphene oxide are characterized by a high transmittance greater than 68% for a wavelength of 550 nm, which creates the possibility of applying these layers in building integrated photovoltaic BIPV (Fig. 30).

3.4. Analysis of the results of electrical and electrochemical studies

The best catalytic properties for the reduction reaction of triiodide to iodide anion characterizes a layer of platinum (Table 4, Fig. 31). The layer of the reduced graphene oxide with PVP coated by the surface of the polymer PEDOT:PSS only slightly increases the resistance of the charge transfer (Fig. 31), so that it can become an alternative to the more expensive platinum. Electrochemical impedance spectroscopy measurements were also allowed to examine the impact of reduced graphene oxide on the electrochemical properties of photoanode. The application of the reduced graphene oxide in semiconductor layer significantly reduces the resistance by increased charge transfer recombination of electrons from the titanium dioxide to FTO (Fig. 32). The reduced graphene oxide forms a two-dimensional structure in titanium dioxide, what increase the rate of charge transfer, thus preventing recombination of the excited electron with the anion triiodide.

The results of measuring of current-voltage characteristics are shown in the Figs. 33 and 34 and are summarized in Table 5, Electrical properties of dye-sensitized solar cells with photoanode with reduced graphene oxide are

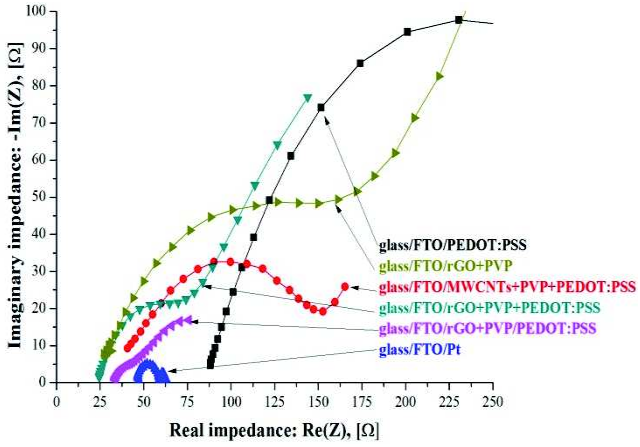

Fig. 31. Nyquist diagrams for the various layers used as a counter electrode of the dye-sensitized solar cells

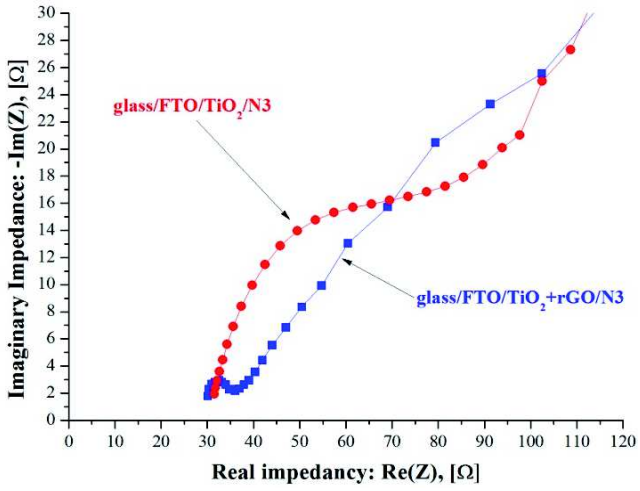

Fig. 32. Nyquist diagrams for the layers of titanium dioxide and titanium dioxide with the reduced graphene oxide deposited on FTO glass and dyed

Table 4.
Charge transfer or recombination resistance R_{CT} of dye-sensitized solar cells layers deposited on FTO glass

Part of the cell	Layer	R_{CT}, Ω
Counter electrode	rGO+PVP	245.6
	rGO+PVP+PEDOT:PSS	52.3
	rGO+PVP/PEDOT:PSS	37.17
	PEDOT:PSS	243.00
	MWCNTs+PVP+PEDOT:PSS	91.63
	Pt	13.6
Photoanode	TiO_2 (dyed)	57.83
	TiO_2 + rGO (dyed)	4.77

better than the electrical properties of cells without reduced graphene oxide (Figs. 33 and 34, Table 5), which was confirmed by measuring their current-voltage characteristics.

As the reference cell, dye-sensitized solar cell with photoanode made of titanium dioxide and a counter electrode made of platinum was used with an efficiency of 4.07% (Fig. 33). Reduced graphene oxide as addition to photoanode with titanium dioxide has a significant impact on the efficiency of dye-sensitized photovoltaic cells. The highest efficiency equal to 4.2% was obtained for the dye-sensitized solar cells with reduced graphene oxide and titanium dioxide as photoanode and platinum counter electrode (Fig. 34). In this case, there is increase in efficiency

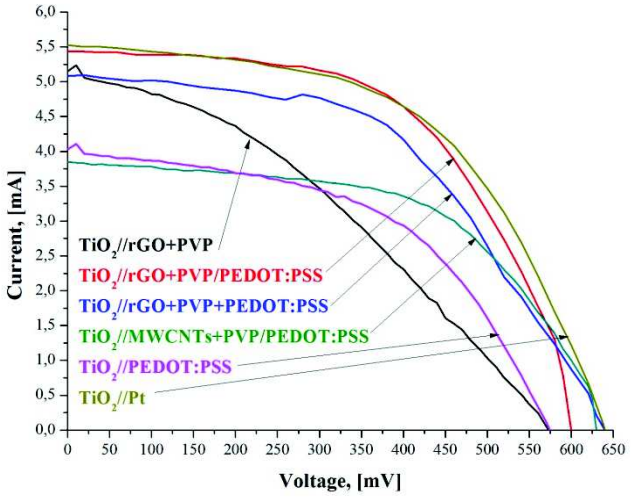

Fig. 33. Current-voltage characteristics of dye-sensitized solar cells with photoanode made of titanium dioxide

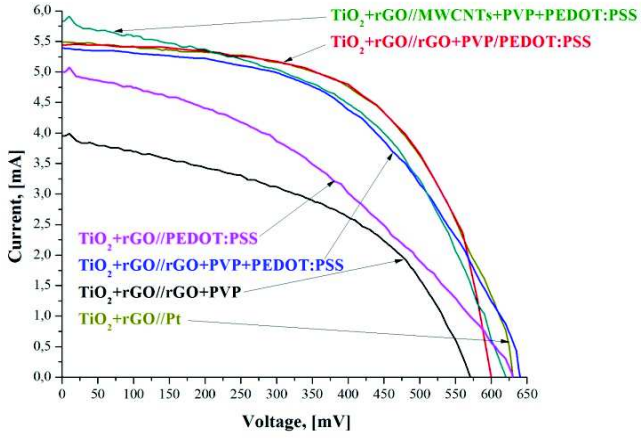

Fig. 34. Current-voltage characteristics of dye-sensitized solar cells with photoanode made of titanium dioxide with the reduced graphene oxide

Table 5.
Summary of electrical properties of experimentally prepared dye-sensitized photovoltaic cells

Material of counter electrode	Electrical properties						
	I_{sc}, mA	U_{oc}, mV	I_{max}, mA	U_{max}, mV	P_m, mW	FF	E_{ff}, %
	Photoanode: TiO_2						
Pt (reference cell)	5.53	639.99	4.39	430.58	1.89	0.53	4.07
PEDOT:PSS	4.03	547.28	2.99	391.90	1.17	0.51	1.85
MWCNTs + PVP + PEDOT:PSS	3.85	629.99	3.13	441.69	1.38	0.57	2.64
rGO + PVP	5.15	573.78	3.36	309.61	1.04	0.35	1.65
rGO + PVP + PEDOT:PSS	5.09	639.99	4.22	394.65	1.66	0.51	3.26
rGO +PVP / PEDOT:PSS on top	5.43	599.99	4.52	412.26	1.86	0.57	3.72
	Photoanode: TiO_2+rGO						
Pt	5.43	599.99	4.45	437.62	1.95	0.60	4.20
PEDOT:PSS	5.00	628.99	3.36	366.02	1.23	0.39	1.94
MWCNTs + PVP + PEDOT:PSS	5.83	620.33	4.27	424.76	1.81	0.50	2.89
rGO + PVP	3.95	571.58	2.63	399.78	1.05	0.46	1.69
rGO + PVP + PEDOT:PSS	5.39	639.99	4.27	414.63	1.77	0.51	3.45
rGO +PVP / PEDOT:PSS on top	5.45	599.99	4.46	438.73	1.96	0.60	3.77

I_{sc} – short-circuit current, U_{oc} – open circuit voltage, I_{max} – current at the point of maximum power, U_{max} – the voltage at the point of maximum power, P_m – the maximum power, FF – the fill factor of characteristics, E_{ff} – the conversion efficiency of solar radiation into electricity

by 0.13% compared to the reference cell. Photovoltaic cells with the counter electrode made of reduced graphene oxide with PVP and conventional photoanode characterizes the lowest efficiency of 1.65% (Fig. 33). Applying a highly conductive polymer – PEDOT:PSS into the reduced graphene oxide with PVP increases the efficiency to 3.26%. For the comparison purposes there was also used a counter with a PEDOT:PSS (Fig. 33) and carbon nanotubes with the addition of PVP and PEDOT:PSS (Fig. 33), where the efficiency were respectively 1.85% and 2.64% for the photoanode without reduced graphene oxide.

The use of the counter electrode with a reduced graphene oxide with PVP coated by the layer of PEDOT:PSS provides an efficiency 3.72% for the conventional photoanode (Fig. 33) and 3.77% for photoanode with reduced graphene oxide (Fig. 34). The results show that the use of reduced graphene oxide in addition to photoanode increases the efficiency of energy conversion of solar radiation into electrical energy, which is indicated also by the results of optical properties. In addition, the results show that it is possible to replace the platinum by reduced graphene oxide and PVP coated by PEDOT:PSS without a significant reduction in electrical properties, with photoanode made of titanium dioxide with a reduced graphene oxide.

4. Conclusions

Insertion to photoanode reduced graphene oxide increases the efficiency of light harvesting and thereby increasing the efficiency of energy conversion of sunlight into electricity by 1.03%. It has also been shown that it is possible to replace the expensive platinum layer, by a layer of the reduced graphene oxide and PVP covered by the layer of highly conductive polymer – PEDOT:PSS, resulting in relatively minimal reduction in efficiency compared to a platinum counter electrode. Increase in efficiency by 0.3% compared to the reference cell and an efficiency of 3.77% for the dye-sensitized solar cell with a reduced graphene oxide and titanium dioxide photoanode and reduced graphene oxide with PVP covered by the layer of PEDOT:PSS as counter electrode, can contribute to reduce the manufacturing costs of the dye-sensitized solar cell.

Development presented in this work: thermal exfoliation of graphene oxide and the production of dye-sensitized solar cells with reduced graphene oxide as both photoanode and counter electrode by applying respectively screen printing method and spin coating method ensures the production of repetitive layers of predetermined thickness without structural defects and impurities.

The results of research and developed technology can offer promise to implement it in mass production, as competition to so far produced dye-sensitized solar cells, mainly due to economic reasons, related to a decrease in the cost of manufacture of such cells as compared to the cells currently manufactured.

Acknowledgements

The project was financed by the National Science Centre granted on the basis of the decision number DEC-2013/09/B/ST8/02943.

References

[1] G. Jastrzębska, Renewable energy sources and environmentally friendly vehicles, WNT, Warsaw 2007.
[2] H. Ellis, Characterization of dye-sensitized solar cells. Components for environmentally friendly photovoltaics, Uppsala University, Dissertation for the Licentiate of Philosophy in Physical Chemistry.
[3] E. Klugmann-Radziemska, Renewable Energy sources, Examples of calculations, Technical University of Gdańsk, Gdańsk, 2006.
[4] J. Zhao, J. Wu, M. Zheng, J. Huo, Y. Tu, Improving the photovoltaic performance of dye-sensitized solar cell by graphene/titania photoanode, Electrochmica Acta 156 (2015) 261-266.
[5] L.A. Dobrzański, A. Mucha, M. Prokopiuk vel Prokopowicz, A. Drygała, K. Lukaszkowicz, Technology of dye-sensitized solar cells with carbon nanotubes, Archives of Materials Science and Engineering 70/2 (2014) 70-76.
[6] J. Nei de Freitas, C. Longo, A. Flavia Nogueria, M.-A. De Paoli, Solar module using dye-sensitized solar cells with a polymer electrolyte, Solar Energy Materials & Solar Cells 92 (2008) 1110-1114.
[7] J. Gong, J. Liang, K. Sumathy, Review on dye-sensitized solar cells (DSSCs): Fundamental concepts and novel materials, Renewable and Sustainable Energy Reviews 16 (2012) 5848-5860.
[8] BP`s Statistical Review of World Energy, 2014.
[9] M. Sokolsky, J. Cirak, Dye-sensitized solar cells: materials and processes, Acta Electrochnica et Informatica 10/3 (2010) 78-81.
[10] T.F. Stocker, D. Qin, G.-K. Plattner, M. Tignor, S.K. Allen, J. Boschung, A. Nauels, Y. Xia, V. Bex, P.M. Midgley, Climate Change 2013: The Physical Science Basis. Contribution of Working Group I to the Fifth Assessment Report of the Intergovernmental Panel on Climate Change, IPCC, Cambridge University Press, Cambridge, UK and New York, NY, USA, 2013.
[11] W.M. Lewandowski, Environmentally friendly renewable energy sources, WNT, Warszawa, 2006.
[12] V. Sugathan, E. John, K. Sudhakar, Recent improvements in dye sensitized solar cells: A review, Renewable and Sustainable Energy Reviews 52 (2015) 54-64.
[13] M. Grätzel, Photoelectrochemical cells, Nature 414 (2001) 338-344.
[14] Y. Jiao, F. Zhang, S. Meng, L.A. Kosyachenko (Ed.), Dye Sensitized Solar Cells Principles and New Design, Solar Cells - Dye-Sensitized Devices, ISBN: 978-953-307-735-2, In Tech 09, 2011.
[15] A. Zdyb, Research on increasing the efficiency of dye-sensitized solar cells, Monographs 94, Polish Academy of Sciences, Committee of Environmental Engineering, Lublin, 2014.
[16] L.A. Dobrzański, A. Drygała, P. Panek, M. Lipiński, P. Zięba, Development of the laser method of multicrystalline silicon surface texturization, Archives of Materials Science and Engineering 38/1 (2009) 5-11.
[17] M. Musztyfaga-Staszuk, L.A. Dobrzanski, S. Rusz, M. Staszuk, Application Examples for the Different Measurement Modes of Electrical Properties of the Solar Cells, Archives of Metallurgy and Materials 59/1 (2014) 247-252.
[18] T. Tesfamichael, G. Will, T. Bostron, J. Bell, Investigations of dye-sensitized titania solar cell electrode using confocal laser scanning microscopy, Journal of Material Science 38 (2003) 1721-1726.
[19] M. Sibiński, T. Stapiński, Z. Lisik, Prospects for the development of technology of thin-film solar cells, Electronics 5 (2013) 40-44.
[20] C.P. Lee, C.A. Lin, T.C. Wei, M.L. Tsai, Y. Meng, C.T. Li, K.C. Ho, C.I. Wu, S.P. Lau, J.H. He, Economical low-light photovoltaics by using Pt-free dye-sensitized solar cell with graphene dot/PEDOT:PSS counter electrodes, Nano Energy (2015) ttp://dx/doi/org/10.1016/j.nanoen.2015.10.008.
[21] M. Kohlstädt, M. Grein, P. Reinecke, T. Kroyer, B. Zimmermann, U. Würfel, Inverted ITO- and PEDOT:PSS free polymer solar cells with high power conversion efficiency, Solar Energy Materials & Solar Cells 117 (2013) 98-102.
[22] X. Yang, M. Xu, W. Qiu, X. Chen, M. Deng, J. Zhang, H. Iwai, E. Watanabe, H. Chen, Graphene uniformly decorated with gold nanodots: in situ synthesis, enhanced dispersability and applications, Journal of Materials Chemistry 21 (2011) 8096-8103.

[23] M. Grätzel, Review: Dye-sensitized solar cells, Journal of Photochemistry and Photobiology C: Photochemistry Reviews 4 (2003) 145-153.
[24] D.W. Zhang, X.D. Li, H.B. Li, S. Chen, Z. Sun, X.J. Yin, S.M. Huang, Graphene-based counter electrode for dye-sensitized solar cells, Carbon 49 (2011) 5382-5388.
[25] H.S. Jang, J.M. Yun, D.Y. Kim, D.W. Park, S.I. Na, S.S. Kim, Moderately reduced graphene oxide as transparent counter electrodes for dye-sensitized solar cells, Electrochimica Acta 81 (2012) 301-307.
[26] Z.Y. Li, M.S. Akhtar, J.H. Kuk, B.S. Kong, O.B. Yang, Graphene application as a counter electrode material for dye-sensitized solar cell, Material Letters 86 (2012) 96-99.
[27] S. Yoon, S. Tak, J. Kim, Y. Jun, K. Kang, J. Park, Application of transparent dye-sensitized solar cells to building integrated photovoltaics systems, Building and Environment 46 (2011) 1899-1904.
[28] R. Corrao, M. Morini, Integration of dye-sensitized solar cells with glassblock, Technical Transactions. Civil Engineering 2-B 3/109 (2012) 55-64.
[29] G. Adinolfi, I. Arsie, R. Di Martino, A. Giustiniani, G. Petrone, G. Rizzo, M. Sorrentino, A Prototype of Hybrid Solar Vehicle: Simulations and On-Board Measurements, Processing of Advanced Vehicle Control Symposium AVEC, Kobe, Japan, 2008.
[30] A. Nikolakopoulou, D. Tasis, L. Sygellou, V. Dracopoulos, C. Galiotis, P. Lianos, Study of thermal reduction of graphene oxide and of its application as electrocatalyst in quasi-solid state dye-sensitized solar cells in combination with PEDOT, Electrochimica Acta 111 (2013) 698-706.
[31] R. Li, Q.Tang, L. Yu, X. Yan, Z. Zhang, Counter electrodes from conducting polymer intercalated graphene for dye-sensitized solar cells, Journal of Power Sources 309 (2016) 231-237.
[32] A. Nikolakopoulou, D. Tasis, L. Sygellou, Dispersion of Graphene in organic solvents and their use for improving efficiency of dye- and quantum dot-sensitized solar cells, Electrochimica Acta 139 (2014) 54-60.
[33] M. Prokopiuk vel Prokopowicz, The impact of reduced graphene oxide on the structure of electrodes and properties of the dye sensitized photovoltaic cells, PhD thesis in progress.
[34] L.A. Dobrzański, M. Prokopiuk vel Prokopowicz, K. Lukaszkowicz, A. Drygała, M. Szindler, Graphene oxide film as transparent counter electrode for dye-sensitized solar cell, Journal of Achievements in Materials and Manufacturing Engineering 73/1 (2015) 13-20.
[35] A.D. Dobrzańska-Danikiewicz, A. Drygała, Strategic development perspectives of laser processing on polycrystalline silicon surface, Archives of Materials Science and Engineering 50/1 (2011) 5-20.
[36] A.D. Dobrzańska-Danikiewicz, Main assumption of the foresight of surface properties formation leading technologies of engineering materials and biomaterials, Journal of Achievements in Materials and Manufacturing Engineering 34/2 (2009) 165-171.
[37] A.D. Dobrzańska-Danikiewicz, Materials surface engineering development trends, Open Access Library 6 (2011) 1-594.
[38] A.D. Dobrzańska-Danikiewicz, Computer integrated development prediction methodology in materials surface engineering, Open Access Library 1/7 (2012) 1-289.
[39] L.A. Dobrzański, M. Szindler, M. Prokopiuk vel Prokopowicz, A. Drygała, K. Lukaszkowicz, T. Jung, M.M. Szindler, Transparent platinum counter electrode for dye-sensitized solar cells, Journal of Achievements in Materials and Manufacturing Engineering 68/1 (2015).
[40] W. Shu, Y.Liu, Z. Peng, K. Chen, C. Zhang, W. Chen, Synthesis and photovoltaic performance of reduced graphene oxide – TiO_2 nanoparticles composites by solvothermal method, Journal of Alloys and Compounds 563 (2013) 229-233.